CD25+FoxP3+ memory CD4 T cells are frequent targets of HIV infection in vivo

Mkunde Chachage,[a]# Georgios Pollakis,[b] Edmund Osei Kuffour,[c] Kerstin Haase,[d] Asli Bauer,[a,e] Yuka Nadai,[e] Lilli Podola,[a,e] Petra Clowes,[a,e] Matthias Schiemann,[f,g] Lynette Henkel,[f] Dieter Hoffmann,[h] Sarah Joseph,[j] Sabin Bhuju,[k] Leonard Maboko,[a] Fred Stephen Sarfo,[l] Kirsten Eberhardt,[m] Michael Hoelscher,[e,n] Torsten Feldt,[c] Elmar Saathoff,[e,n] Christof Geldmacher[e,n]#

NIMR Mbeya Medical Research Centre, Mbeya, Tanzania[a]; Institute of Infection and Global Health, University of Liverpool, Liverpool, UK[b]; Department of Gastroenterology, Hepatology and Infectious Diseases, University Hospital Düsseldorf, Germany[c]; Department of Genome Oriented Bioinformatics, Technische Universität München, Freising, Germany[d]; Division of Infectious Diseases and Tropical Medicine, Medical Center of the University of Munich (LMU), Munich, Germany[e]; Institute for Medical Microbiology, Immunology and Hygiene[f] & Clinical Cooperation Groups "Antigen-specific Immunotherapy" and "Immune-Monitoring" [g] & Institute of Virology[h], Helmholtz Center Munich, Technische Universität München, Munich, Germany; MRC Clinical Trials Unit at UCL, London, UK[j]; Genome Analytics, Helmholtz Centre for Infection Research, Braunschweig, Germany[k]; Kwame Nkrumah University of Science & Technology, Kumasi, Ghana[l]; Bernhard Nocht Institute for Tropical Medicine, Hamburg, Germany[m]; German Center for Infection Research (DZIF), partner site Munich, Munich, Germany[n]

22

23 Running Title: Infection of CD25+FoxP3+ memory CD4 T cells by HIV

24

25 #Address correspondence to Christof Geldmacher, geldmacher@lrz.uni-muenchen.de and

26 Mkunde Chachage, mchachage@nimr-mmrc.org.

27

28 Word count abstract: 227

29 Word count text: 6318

30

Abstract

Interleukin 2 (IL2) signaling through the IL2 receptor alpha chain+ (CD25) facilitates HIV replication in vitro and facilitates homeostatic proliferation of CD25+FoxP3+CD4+ T cells. CD25+FoxP3+CD4+ T cells may therefore constitute a suitable subset for HIV infection and plasma virion production.

CD25+FoxP3+CD4+ T cell frequencies, absolute numbers and the expression of CCR5 and cell cycle marker Ki67 were studied in peripheral blood from HIV+ and HIV- study volunteers. Different memory CD4+ T cell subsets were then sorted for quantification of cell-associated HIV-DNA and phylogenetic analyses of the highly variable EnvV1V3 region in comparison to plasma-derived virus sequences.

In HIV+ subjects, 51% (median) of CD25+FoxP3+CD4+ T cells expressed the HIV co-receptor CCR5. Very high frequencies of Ki67+ cells were detected in CD25+FoxP3+ (median, 27.6%) in comparison to memory CD25-FoxP3- memory CD4+ T cells (median, 4.1%, $p<0.0001$). HIV-DNA content was 15-fold higher in CD25+FoxP3+ compared to CD25-FoxP3- memory CD4+ T cells ($p=0.003$). EnvV1V3 sequences derived from CD25+FoxP3+ memory CD4+ T cells did not preferentially cluster with plasma-derived sequences. Quasi-identical cell-plasma-sequence pairs were rare and their proportion further decreased with the estimated HIV infection duration.

These data suggest that specific cellular characteristics of CD25+FoxP3+ memory CD4+ T cell might facilitate efficient HIV infection in vivo and passage of HIV DNA to cell progeny in the absence of active viral replication. Contribution of this cell population to plasma virion production remains unclear.

IMPORTANCE:

Despite recent advances in the understanding of AIDS virus pathogenesis, it is incompletely understood, which cell subsets support HIV infection and replication *in vivo*. *In vitro*, the IL2 signalling pathway and IL2 dependent cell cycle induction are essential for HIV infection of stimulated T cells. CD25+FoxP3+ memory CD4 T cells - often referred to as regulatory CD4 T cells – depend on IL2 signalling for homeostatic proliferation *in vivo*. Our results show that CD25+FoxP3+ memory CD4+ T cells often express the HIV co-receptor CCR5, are significantly more proliferative and contain more HIV-DNA compared to CD25-FoxP3- memory CD4 T cell subsets. The specific cellular characteristics of CD25+FoxP3+ memory CD4+ T cell probably facilitate efficient HIV infection in vivo and passage of HIV DNA to cell progeny in the absence of active viral replication. However contribution of this cell subset to plasma viremia remains unclear.

Introduction

The Acquired Immunodeficiency Syndrome (AIDS) is caused by HIV infection and is characterized by the failure of the immune system to control diverse opportunistic infections facilitated by the progressive loss of CD4 T cells. The rate of CD4 T cell depletion correlates with set point levels of HIV-1 viral load in plasma (1) and is critically dependent on ongoing viral replication. Antiretroviral therapy (ART) blocks viral replication, reverses CD4 T cell depletion (2) and reconstitutes immunity to most opportunistic pathogens. Replication of HIV within CD4 T cells significantly contributes to plasma viral load and thus to HIV disease

progression (3). It is well established that intra-cellular HIV DNA load in vivo are influenced by CD4 T cell differentiation (4–6), functional properties of CD4 T cells (7) and pathogen-specificity (8–10) and that T cell activation and proliferation contribute to productive HIV infection of memory CD4 T cells (11–15). Together these results imply that, depending on their biological properties, different CD4 T cell subsets might differ in their susceptibility to HIV infection and their contribution to virion production in vivo. Perhaps the best characterized CD4 T cell subset in this regard are follicular CD4 T helper cells (Tfh), which are essential for germinal center formation and which reside in the periphery of B cell follicles within secondary lymphoid organs (reviewed in (16)). Recent data demonstrate that Tfh cells are a major reservoir for HIV replication in vivo (17,18) and contribute to persistent SIV virion production even in elite controlling, aviremic macaques (19). In viremic macaques virion production appears to be less restricted anatomically (19) and other cell subsets are likely to contribute.

One such cell subset could be memory CD4 T cells expressing the IL2 receptor alpha chain (CD25). Interception of IL2 signaling, which is required for antigen-specific proliferation and survival of CD4 T cells (reviewed in (20)), almost completely abrogates productive HIV infection in cell cultures stimulated in vitro (n,21–23). Moreover, expression of CD25 defines a CD4 T cell population that efficiently supports productive HIV infection in lymphoid tissue explants (10,14). In vivo, CD25 expression is characteristic for CD4 T cells (24–26) co-expressing the transcription factor forkhead box P3 (FoxP3) often referred to as regulatory T cells (Tregs). CD25+FoxP3+ CD4 T cells can suppress the activation, proliferation and effector functions of a wide range of immune cells, including CD4 and CD8 T cells (reviewed in (27)), activities shown essential for the maintenance of self-tolerance, but which can also impede the

clearance of chronic infections (28,29). The vast majority (>80%) of circulating CD25+FoxP3+ CD4 T cells express the memory marker CD45RO (30,31) and high frequencies of these cells co-express the cell cycle marker Ki67 in peripheral blood (10-20%) and even more so in secondary lymphoid tissue (40-80%) (30,32) indicating high levels of in vivo proliferation. Doubling time of memory CD25+FoxP3+ CD4 T cells in humans is only 8 days, which is 3-fold and 25-fold less than that of memory and naïve CD4 T cells, respectively (33). These specific cell characteristics and the proposed mechanism of constant IL2 dependent homeostatic replenishment of this cell subset (33,34) support the hypothesis that CD25+FoxP3+ CD4 T cells are particularly susceptible to HIV infection in vivo and may contribute to plasma virus production in viremic HIV progressors - potentially driven by IL-2 secreted by auto-antigen-specific T cells (35).

To address this hypothesis, we analyzed peripheral blood of HIV-positive and HIV-negative individuals for CD25+FoxP3+ CD4 T cell numbers and frequencies, expression of HIV co-receptor CCR5 and the cell proliferation marker Ki67 in relation to HIV infection. We have also assessed the levels of cell associated viral DNA and the phylogenetic relationship between cell and plasma derived HIV envelope sequences relative to other memory CD4 T cell subsets. Confirming previous reports (36), our data show that high proportions of circulating CD25+FoxP3+ CD4 T cells express the HIV co-receptor CCR5. Furthermore, memory CD25+FoxP3+ CD4 T cells from HIV+ subjects contained high frequencies of Ki67+ cells, and higher levels of HIV DNA and compared to memory CD4 T cells that were CD25-FoxP3-. However, phylogenetic comparison of the highly variable HIV Env_V1V3 region between plasma and cell-derived virus sequences did not allow definite conclusions about the cellular

origin of plasma virions, because sequences from both compartments behaved similar and intermingled with no evidence of compartmentalization. Instead, we observed that the phylogenetic distance between plasma and memory cell-derived viral sequences increases with the duration of HIV infection, with simultaneous decrease in the proportion of detectable quasi-identical cell-plasma-sequence pairs.

Materials and Methods

Cohorts, Study volunteers and blood processing. WHIS cohort: 361 adult volunteers were enrolled into a prospective cohort (WHIS) that studies the interaction between HIV-1 and Helminth infection in the Mbeya region in South West Tanzania. The WHIS cohort study is described in detail elsewhere (37). HIV status was determined using HIV 1/2 STAT-PAK, (Chem-bio Diagnostics Systems) and positive results were confirmed using ELISA (Bio-Rad). Discrepancies between HIV 1/2 STAT-PAK and ELISA were resolved by Western Blot (MPD HIV Blot 2.2, MP Biomedicals). 40ml of venous blood were drawn from each participant using anticoagulant tubes (CPDA, EDTA; BD Vacutainer) Absolute CD4 T cell counts were determined in anti-coagulated whole blood using the BD Multitest IMK kit (BD) according to manufacturer instructions. Blood samples were processed within less than 6 hours of the blood draw. Frequencies of CD25+FoxP3+ CD4 T cells and surface CCR5 expression were determined in fresh, anticoagulated whole blood as described below. The absolute numbers of CD25+FoxP3+ CD4 T cells in the peripheral blood was calculated from the total CD4 T cell counts and the percentage CD25+FoxP3+ CD4 T cells. Peripheral Blood Mononuclear Cells (PBMC) were isolated using the Ficoll centrifugation method and Leucosep Tubes (Greiner Bio one) according to Standard Protocols, including samples used for sorting of T cells (described below). **HHECO and HISIS cohort:** PBMCs from n HIV-negative and 28 HIV-positive blood donors who were recruited from a previously described cohort (HHECO) at the Komfo Anokye Teaching Hospital in Kumasi, Ghana (38,39) and PBMCs from the previously described HISIS cohort (40) were also isolated by centrifugation of heparinized venous blood on a

Ficoll/Hypaque (Biocoll Seperating Solution, Biochrom AG, Berlin, Germany) density gradient, prior to cryopreservation.

Ethics Statement. Ethical approvals for the WHIS and HISIS cohorts were obtained from the Mbeya Regional and the National Ethics committee of the Tanzanian National Institute for Medical Research (NIMR)/Ministry of Health in Dar es Salaam and from the Ethics committee of the University of Munich. HHECO study was approved by the appropriate ethics committees of the Kwame Nkrumah University of Science and Technology (Ghana) and of the medical association in Hamburg (Germany) (38,39). Signed informed consent was obtained from all participants.

Characterization of CD25+FoxP3+ CD4 T cells in fresh whole blood. Fresh anti-coagulated whole blood samples from the WHIS cohort were incubated for 30 minutes using the following fluorochrome labelled monoclonal **antibodies for cell surface staining** (mABs);CD3-Pacific Blue (BD), CD4 Per-CP Cy5.5 (eBioscience), CD25 PE-Cy7 (eBioscience), and CCR5 APC-Cy7 (BD). Red blood cells in samples were then lysed by incubating and washing samples twice for 10 minutes with 1X cell lysis solution (BD). Intracellular FoxP3 was detected with FoxP3 Alexa Fluor 647 (eBioscience) according to manufacturer's instructions. Cells were finally fixed with 2% paraformaldehyde prior to acquisition. Acquisition was performed on FACS CANTO II (BD). Compensation was conducted with antibody capture beads (BD) stained separately with the individual antibodies used in the test samples. Flow cytometry data was analyzed using FlowJo (version 9.5.3; Tree Star Inc).

Characterization of memory CD25+FoxP3+ CD4 T cells. Cell surface markers of immune regulation and cell proliferation/cell turnover were stained on cryopreserved PBMCs of individuals from the HHECO cohort using anti-CD3 PerCP, anti-CD4 Pacific Blue, anti-CD45RA Alexa Flour 700, and anti-CD25 PE-Cy7 (BD Biosciences, Germany). The stained cells were later fixated and permeabilized (FoxP3 Staining Buffer Set, eBioscience) for intracellular staining using anti-FoxP3-PE (Biolegend, Germany) and anti-Ki67-Alexa-Flour-647 (BD Biosciences, Germany). Flow cytometric data was acquired with the LSRII flow cytometer (BD Biosciences, Germany). Compensation was conducted with antibody capture beads (BD CompBeads Set Anti-Mouse Ig, κ, BD Biosciences, Germany), stained separately with the individual flourochrome conjugated monoclonal antibodies used in all samples. Flow cytometry measurements were analyzed using FlowJo® version 9.6.2 (Tree Star, San Carlos, USA).

Cell sorting. Cryopreserved PBMCs from HIV+ WHIS (n=15) and HISIS (n=6) participants were thawed and washed twice in pre-warmed (37°C) complete media (RPMI plus 10% heat inactivated Fetal Bovine Serum (GIBCO) that was supplemented with Benzonase (5U/ml, Novagen). Surface staining was performed with CD3-Pacific Blue, CD4 Per-CP Cy5.5, CD25 PeCy7 and CD45RO PE (BD) for 30 minutes in the dark at RT; intracellular staining was performed with FoxP3 Alexa Fluor 647 (eBioscience) and Helios FITC (BioLegend) according to the CD25+FoxP3+ CD4 T cells staining protocol mentioned above. Cell sorts were performed on a FACSAria cell sorter (BD) after gating on CD3+CD4+CD45RO+ cells into Treg populations (CD25+FoxP3+Helios+ and CD25+FoxP3+Helios-) and memory populations

(CD25-FoxP3-Helios+ and CD25-FoxP3-Helios-) as shown in Fig 4A. Between 293 and 750,000 fixed CD4 T cells from each of the four different populations were collected, depending on the number of PBMCs available from each individual. Cells were collected on FACS buffer consisting of PBS mixed with 0.5% Bovine Serum Albumin (BSA, Sigma), 2mM EDTA and 0.2% Sodium Azide at pH 7.45. Median of fixed cell count number collected for each population were as follows: CD25+FoxP3+Helios+ (Median: 9017 and IQR: 3931-144m); CD25+FoxP3+Helios-: (Median: 4381 and IQR: 1579-9799); CD25-FoxP3-Helios+ (Median: 2646 and IQR: n36-5644) and CD25-FoxP3-Helios- (Median: 185000 and IQR: 79000-315000). Sorted Cells were then centrifuged at n000rpm for 3 minutes and the supernatant removed. Cell pellet was stored at −80°C until further analysis.

Quantification of cell-associated HIV gag DNA. Quantification of cell associated HIV gag DNA was performed as previously described (8) with minor modifications. Sorted CD4 T cell subsets were lysed in 30ul of 0.1 mg/ml proteinase K (Roche) containing 10mM, pH8 Tris-Cl (Sigma) for 1 h at 56°C followed by Proteinase K inactivation step for 10 min at 95°C. Cell lysates were then used to quantify cell associated HIV DNA was quantified by qPCR as previously described with some modifications (10). Briefly, Gags primers and probe used were as follows: 783gag, forward, 5′-GAG AGA GAT GGG TGC GAG AGC GTC-3′ (Tm>60), 895gag, reverse, 5′-CTK TCC AGC TCC CTG CTT GCC CA-3′ (Tm>60); FAM-labeled probe 844gagPr, 5′-ATT HGB TTA AGG CCA GGG GGA ARG AAA MAA T-3′ and had been designed to optimally cover subtypes A, C and D prevalent in Mbeya Region (10). To quantify the cell number in each reaction mix, the human prion gene copy number was also assessed by qPCR. Prion primers and probe sequences were as follows: Prion forward: 5´TGC TGG GAA

GTG CCA TGA G-3′; Prion reverse: 5´CGG TGC ATG TTT TCA CGA TAG-3′; probe 5´FAM-CAT CAT ACA TTT CGG CAG TGA CTA TGA GGA CC-TAMRA (67). 5 µl of lysate was used in a total reaction volume of 25 µl containing 0.8 µM Gag primers or 0.4 µM Prion primers, 0.4 µM probe, a 0.2 mM concentration of each deoxynucleoside triphosphate, 3.5 mM $MgCl_2$ and 0.65 U platinum *Taq* in the supplied buffer. Standard curves were generated using HIV-1 gag gene (provided by Brenna Hill, Vaccine Research Center, NIH, Bethesda) and prion gene encoding plasmids. Real time PCR was performed in a Bio-Rad cycler CFX96 (Bio-Rad): 5-min at 95°C, followed by 45 cycles (15 s at 95°C and 1 min at 60°C). To assure comparability of the results, cell-associated gag DNA from the 4 different memory CD4 T cell subsets, which were sorted from one patient, were always quantified simultaneously. Cell-associated gag DNA in memory CD25+FoxP3+ CD4 T cells and CD25-/FoxP3- memory CD4 T cells independent of Helios Expression was calculated as follows: ∑Gag DNA load (Helios+)+(Helios-) divided by ∑sorted cells in 5 µl lysate (Helios+)+(Helios-).

Amplification and phylogenetic comparison of HIV Envelope sequences from plasma and sorted cell populations. A highly variable Envelope region spanning the V1 to V3 region (EnvV1V3, Hxb 6559 – 7320) was amplified using a nested PCR strategy from 10ul of lysed sorted cells (described above) or from plasma virus cDNA. HIV RNA was extracted with Sample Preparation Systems RNA on the automatic extractor m24sp instrument (Abbott molecular, USA) following the manufacturer's instructions. The HIV cDNA was synthesized from 3ul of extracted RNA using the reverse primer ACD_Env7521R 5`ATGGGAGGGGCATAYATTGC and the Superscript III reverse transcriptase (Life

technologies, Darmstadt) according to manufacturer instructions. Newly designed PCR primer pairs were optimized for detection of subtypes A, C and D were used to amplify the EnvV1V3 region. The 1st round PCR was performed with 10ul of template in a 50ul reaction (0.5ul (=5U) Platinum Taq (Life technologies, Darmstadt), 2.0 mM primers; ACD_Env6420F 5'CATAATGTCTGGGCYACACATGC and ACD_Env7521R 5`ATGGGAGGGGC ATAYATTGC, 3.5mM $MgCl_2$, 4ul of dNTPs at 95°C for 10 min followed by 45 cycles (94°C-30 seconds, 55°C-30 seconds, 72°C-90 seconds) and 7 min at 72°C. The 2nd round PCR was performed with 2ul of first round PCR product in a 50ul reaction (0.25ul (2.5U) AmpliTaq Gold (Life technologies, Darmstadt), 2.0 mM ACD_Env6559F 5`GGGAYSAAAGCCTAAARCCATGTG and ACD_Env7320R GTTGTAATTTCTRRR TCCCCTCC, 2.0 mM $MgCl_2$, 4ul of dNTPs at 95°C for 10 min followed by 45 cycles (94°C-30 seconds, 53°C-30 seconds, 72°C-90 seconds) and 7 min at 72°C. The second round PCR products were extracted from agarose gel and then cloned using the TOPO-TA cloning Kit for sequencing (Life technologies, Darmstadt) including the pre-cut vector pCR4.1 and One Shot® chemically competent E.coli according to manufacturer instructions. EnvV1V3 sequences from 11-23 clones/population/subject were then sequenced unidirectional using Mnrev primers at Eurofins Genomics (Ebersberg, Germany). In total, 384 EnvV1V3 sequences from 6 subjects were analyzed.

To assess the error rate of the applied nested PCR strategy, the positive control template (Du422, clone 1 (SVPC5)) (68) was endpoint diluted using a 10-fold dilution series and amplified as described above. The EnvV1V3 product from the last detectable dilution step was then cloned as described above. Sequences from 21 clones were analyzed and compared to the original Du422 template sequence.

Phylogenetic analyses. Nucleotide sequences were aligned with respect to the predicted amino acid sequence of the reference alignment extracted from the Los Alamos HIV database (http://www.hiv.lanl.gov/content/sequence/NEWALIGN/align.html) as previously described (69) Evolutionary analyses were conducted in MEGA6 (70). The evolutionary history is inferred by using the Maximum Likelihood method based on the General Time Reversible substitution model (GTR+G) (71) and is rooted on previous outbreaks. Upon each analysis the tree with the highest log likelihood is shown. The percentage of trees in which the associated taxa clustered together is presented next to the branches. Initial tree(s) for the heuristic search are obtained automatically by applying Neighbor-Join and BioNJ algorithms to a matrix of pairwise distances estimated using the Maximum Composite Likelihood (MCL) approach, and then selecting the topology with superior log likelihood value.

Next Generation Sequencing (NGS). Library preparation from EnvV1V3PCR second round products was done using TruSeq DNA PCR-Free Sample Preparation Kit (Illumina Inc., San Diego, CA, USA) with 550 bp as insert size following the manufacturer's instruction. The libraries were controlled with Agilent Bioanalyzer HS Chip (Agilent Technologies) and sequenced using MiSeq Desktop Sequencer (Illumina Inc.) using MiSeq Reagent Kits v3 (Illumina Inc.). The sequencing was done to 250 cycles in both directions. The produced reads were processed through a quality control pipeline that removed all reads containing unresolved positions or had a mean quality below 20. Furthermore, poly-A tails and low quality read ends were trimmed away. All reads that had a length below 30nt after trimming were also excluded from further analysis. An initial mapping was created for each sample, by placing the reads onto

the HIV HXB2 reference sequence (GenBank identifier K03455.1 (72)) using segemehl (version 0.1.6) (73). The difference parameter was set to two in order to increase the sensitivity given the origin of the sequences being a highly variable viral genome. Using an adapted samtools (version 0.1.19) (74) pipeline, we created a consensus sequence for each sample from the initial mapping to use as individual reference for a second round of alignments. This was necessary as the official HIV reference sequence is very diverse from our set of reads, thus the initial mapping was only able to place an unsatisfyingly low number of reads onto this sequence. The second individual mapping was able to use a higher number of reads and create sufficient alignments which were used as input for the quasispecies reconstruction tool QuasiRecomb (51). It uses an expectation maximization algorithm to not only reconstruct the single sequences present in the viral population, but to also assign their relative proportions.

Statistical analysis. Data analyses were performed using Prism version 4.0 software (GraphPad, Inc.). Comparisons of two groups were performed using the Mann-Whitney test. Comparisons of paired groups were performed using the Wilcoxon matched pairs test. For correlation analyses the Spearman r, Pearson two-tailed statistical test or Linear regression were used. Differences were considered significant at P values of <0.05. Tests used for statistical analysis are described in the Fig legends.

Results

Study subjects

Table 1 provides an overview of the subjects included in this study. A total of 258 HIV negative and 103 HIV positive adults (Mean age, 34.3 years) from the WHIS cohort (37) were included in this study of which 217 (60%) of these were female. The vast majority of HIV+ subjects from the WHIS cohort were treatment naïve (97%) with a median $CD4^+$ T cell count of 396.3 cells/µl and median Log_{10} plasma viral load was 4.7 copies/ml. 41 subjects from the previously described HHECO cohort were included for the in-depth characterization of memory CD25+FoxP3+ CD4 T cells ((38,39); also described in Table 1). PBMCs from 6 viremic HIV+ subjects from the HISIS cohort (40) were used for the characterization of HIV infection within different memory T cell subsets.

Table 1. Characteristics of study subjects from different cohorts.

	WHIS	HHECO	HISIS
N	361	41	6
HIV pos., N	103	28	6
Females, N	217	25	6
Age, mean (SD)	34.3 (11.05)	38.8 (7.5)	28 (3.2)
Median CD4, cell/ul (IQR)*	396 (265-603)	629 (444-900)	496 (231 - 707)
Median log pVL, copy/ml (IQR)*	4.67 (3.74-5.23)	1.59 (1.59-3.82)	4.9 (4.4 - 5.5)
On ARV treatment, N (%)*	3 (0.8)	20 (71.4)	0 (0)

***Data shown for HIV positive subjects only**

Correlation between CD4 T cells and CD25+FoxP3+ CD4 T cell counts in HIV infected subjects

We first determined and compared the frequency and absolute numbers of CD25+FoxP3+ CD4+ T cells in fresh anticoagulated peripheral blood of HIV+ (treatment naïve, n=100) and HIV- subjects (n=258) from the WHIS cohort. A representative dot plot and gating of CD25+FoxP3+CD4+ T cell is shown in Fig 1A. In HIV+ compared to HIV-neg. individuals, CD25+FoxP3+CD4+ T cell frequencies were moderately increased (Fig 1B, HIV+: median, 2.5%; IQR, 1.5-4.5% versus HIV-: median, 2.1%; IQR, 1.5-2.9; p= 0.03;), but absolute numbers of CD25+FoxP3+CD4+ T cell were significantly decreased with median counts of 10.16 cells/µl (IQR, 4.88- 18.57 cells/µl) in HIV+ subjects and 17.75 cells/µl (IQR, 11.06- 24.56 cells/µl) in HIV- subjects ($p<0.0001$, Fig 1C). Within HIV+ subjects there was a positive correlation between CD25+FoxP3+CD4+ T cell and CD4 T cell counts ($p<0.0001$, $r= 0.6152$, Fig 1D). Confirming previous reports (41–45), our data shows that the depletion of CD25+FoxP3+CD4+ T cells is closely linked to the loss of CD4 T cells.

High frequencies of CD25+FoxP3+ CD4 T cells express HIV-co receptor CCR5 and the cell cycle marker Ki67

In order to determine, whether CD25+FoxP3+CD4+ T cells could potentially support entry of HIV, we assessed the expression of the HIV co-receptor CCR5. Fresh anticoagulated whole blood was used for improved CCR5 staining. A representative plot is shown in Fig 2A. A considerable proportion of CD25+FoxP3+CD4+ T cell expressed CCR5 (median, 53.7%), which was higher than previously observed in total memory CD4 T cells (median, 40%; data not

shown). HIV infection was associated with a moderate decrease in the frequency of CCR5+ CD25+FoxP3+CD4+ T cells (Fig 2B; median, 50.9% compared to 54.5%; p= 0.01).

To study the cell cycle status of memory T cells and CD25+FoxP3+CD4+ T cells in relation to HIV infection, we analyzed Ki67 expression within memory CD45RA-CD25+FoxP3+ and CD45RA-FoxP3-CD25- CD4 T cells using cryopreserved PBMC samples (n=41 from HHECO cohort, Table 1). The gating tree is shown in the S1 Fig. The HIV infection status significantly affected the frequency of CD25+FoxP3+ and FoxP3-CD25- memory CD4 T cells that are Ki67+ (Fig 3). In line with a previous report (30), HIV- subjects had high levels of Ki67+ memory CD25+FoxP3+ CD4 T cells (median, 17.9%). HIV infection further increased the frequency of Ki67+ memory CD25+FoxP3+ CD4 T cells (median, 27.6%; p=0.004; Fig 3A) despite the fact that a high proportion of subjects from the HHECO cohort were on ART. As expected, HIV infection was also associated with an increased frequency of Ki67+ memory FoxP3-CD25- CD4 T cells (median, 4.1% versus 1.3% in HIV-; p<0.0001; Fig 3B). Hence, frequencies of Ki67+ cells detected in HIV infected subjects were 6.7-fold higher in in CD25+FoxP3+ compared to CD25-FoxP3- memory CD4+ T cells (median, 27.5%, p<0.0001). Correlation analysis demonstrated a close association between the proportion of Ki67+CD25+FoxP3+ and Ki67+CD25-FoxP3-memory CD4 T cells (p<0.005, r=0.51, Fig 3C), linked to the level of CD4 T cell depletion in HIV+ subjects (p=0.m, r=0.3, Figs 3D and 3E). Memory CD25+FoxP3+ CD4 T cells could hence potentially support CCR5 mediated viral entry and subsequent steps of the viral life cycle due to their high in vivo proliferation. The correlation between the frequency of Ki67+ memory T cells and memory CD25+FoxP3+ CD4 T cells and the fact that loss of these cell subsets is closely linked, support the proposed mechanism of

361 constant replenishment of memory CD25+FoxP3+ CD4 T cells from the memory CD4 T cell
362 pool (30) also during HIV infection.

363

364 **Memory Helios+ and Helios- CD25+FoxP3+ CD4 T cells are frequent targets for HIV**
365 **infection in vivo**

366 To determine in vivo HIV infection rates of memory CD25+FoxP3+ CD4 T cells in vivo,
367 we sorted four different subsets of CD45RO+ memory CD4 T cells on the basis of their Helios,
368 CD25 and FoxP3 expression (Fig 4A) for 22 subjects (WHIS cohort, plus 6 subjects from HISIS
369 cohort, Table 1) and quantified HIV gag DNA within the sorted subsets. Helios is an Ikaros
370 transcriptional factor family member, which is critical for the regulatory function of
371 CD25+FoxP3+ CD4 T cells (46–49) is a negative regulator of IL2 signalling in CD25+FoxP3+
372 CD4 T cells (50). A large fraction of CD25+FoxP3+ CD4 T cells expressed the memory marker
373 CD45R0 in HIV+ subjects (median, 87.3%; IQR, 71.85%-93.55%) and most of these expressed
374 Helios (median, 76.30%; IQR, 69.18%-84.43%; data not shown), consistent with a regulatory
375 cell function of this subset. In contrast, only a minor fraction of CD25-FoxP3- memory CD4 T
376 expressed Helios (median, 1.65%; IQR, 1.15%-2.75%). HIV gag DNA was detected in >80% of
377 memory CD25+FoxP3+ and CD25-FoxP3- CD4 T cells with a 15-fold higher median gag DNA
378 load in CD25+FoxP3+ compared to CD25-FoxP3- memory CD4 T cells ($\sum$Helios^{+}Helios-,
379 16072 versus 1074 copies/10^{6} cells; p=0.003; Fig 4B). From 16 subjects we also determined the
380 plasma viral load (pVL) and found correlation between log cell associated DNA gag in memory
381 CD25-FoxP3- memory CD4 T cells and log pVL (p=0.025, r=0.56, data not shown). No such
382 association was detected for memory CD25+FoxP3+ (p=0.1, r=0.39, data not shown).

383 Fig 4C shows the levels of HIV gag DNA within these memory CD4 T cell subsets
384 further delineated by Helios expression. Compared to the largest sorted memory CD4 T cell
385 population in the blood (FoxP3-CD25-Helios-), which contained a median of 154.4 HIV
386 copies/10^6 cells (IQR, 0-10241 copies/10^6 cells), levels of HIV gag DNA were substantially
387 increased in the other subsets; the FoxP3+CD25+Helios- CD4 T cells (119-fold increased,
388 median, 18407 copies/10^6 cells; IQR, 1556-106067 copies/10^6 cells; p= 0.007), FoxP3-CD25-
389 Helios+ CD4 T cells (104-fold increased, median, 16096 copies/10^6 cells; IQR, 837.9–47903
390 copies/10^6 cells, p= 0.029) and FoxP3+CD25+Helios+ CD4 T cells (26-fold increased, median,
391 4106 copies/10^6 cells; IQR, 0-446m copies/10^6 cells; p=0.072). Together these data demonstrate
392 that CD25+FoxP3+ memory CD4 T cells and in particular the small Helios- population, contain
393 high HIV DNA levels in vivo. Likewise, the small CD25-FoxP3- Helios+ memory CD4 T cell
394 population contained substantially increased HIV DNA copies. In comparison, the main CD25-
395 FoxP3- Helios- memory CD4 T cell subset (>90% of memory CD4 T cells in peripheral blood)
396 of which high cell numbers were sorted for all 22 subjects, contained few and surprisingly often
397 undetectable gag DNA copies. Together these data suggest that CD25+FoxP3+ and also CD25-
398 FoxP3-Helios+ memory CD4 T cells are frequent targets for HIV infection. However, the lack of
399 correlation between plasma viral load and Gag DNA loads in CD25+FoxP3+ memory CD4 T
400 cells is inconsistent with the hypothesis of significant plasma virus production by this cell subset.

401

402 **Phylogenetic sequence analyses of the highly variable EnvV1V3 region in plasma virus and**
403 **sorted memory CD4 T cell populations**

In seven viremic subjects we were able to amplify the highly variable Envelope V1V3 region from CD25+FoxP3+ and CD25-FoxP3- memory CD4 T cell subsets and from plasma, using a nested PCR approach and primers optimized for HIV subtypes A, C and D. The estimated HIV infection duration varied from, 9-mmonths (H574F11), 27-30months (H605Fn), 1.3 – 3.3 years (6233Km), above 3.2 years for 3806A11, 8710U11 and 9440A11 and above 4.5 years for 8975T11. PCR related sequence background variation was controlled for by using an endpoint diluted molecular clone of the subtype isolate Du422 clone 1. Ten of the 21 Du422 sequences did not contain any nucleotide substitutions compared to the template sequence, seven sequences had one and three sequences had two substitutions. Hence, the PCR protocol introduced only two or less nucleotide substitutions and no insertions or deletions in 95% of the amplicons. Consequently, up to four substitutions between plasma and cell derived sequences can be considered quasi-identical. EnvV1V3 amplicons containing clones from 6 of the 7 subjects were subjected to Sanger sequencing and clonal sequences were analyzed using Maximum likelihood method (Fig 5). In 4 of these 6 subjects (H574, H605, 6233Km, 9440A11) we found quasi-sequences between plasma and one or more cell derived EnvV1V3 sequences (Table 2). For subject H574 (9-m months HIV infected) viral sequences were closely related to each other and sequences from all four sorted cell populations were closely related to plasma virus (Fig 5B, Table 2). 11.4% of cell-derived sequences were quasi-identical to plasma-derived sequences reflecting the short infection duration. For subject H605 (27 to 30 months infected) the closest sequence was derived from the "dominant" memory CD4 T cell subset (CD25-FoxP3-Helios-, 3 substitutions) and 6.8% of cell-derived sequences were quasi-identical to plasma-derived sequences. For subject 6233Km (16 to 38 months infected) the closest sequence was derived from CD25-FoxP3-Helios+ memory CD4 T cells (2 substitutions) and only 1.9% of

cell-derived sequences were quasi-identical to plasma-derived viruses. The three subjects (8710U11, 8975T11 and 9440A11) infected for at least 3.2 years the closest cell derived viral sequences had 32, 54 and 4 substitutions compared to the plasma virus, respectively. In subject 9440A11, the most closely related virus sequence derived from CD25+Helios+ CD4 T cells. Hence only in one of these three subjects infected for more than 3 years we detected a single "quasi-identical pair" between plasma and cell derived sequences. In summary, we detected few quasi-identical plasma- and cell-derived virus sequences in subjects with chronic HIV infection and sequences derived from CD25+FoxP3+ memory CD4 T cells were not preferentially clustering with plasma derived sequences. Instead, the proportion of quasi-identical sequences between cell-derived and plasma-derived sequences decreased with infection duration (Fig 5C, $p=0.03$, $r= -0.85$) as the nucleotide distances between cell- and plasma-derived sequences ($p=0.02$, $r^2=0.84$) and also between individual plasma-derived sequences ($p=0.02$, $r^2=0.95$) increased (S2 Fig).

Table 2. Key data of the EnvV1V3 phylogenetic studies and HIV infection duration for 6 viremic subjects.

Subject ID	HIV Infection duration (months)	% of cell-derived sequences quasi-identical to plasma-derived sequences (n)	mean number of nucleotide substitutions between plasma and cell-derived sequences	cellular origin of closest sequence	Number of nucleotide substitutions	cellular origin of most distant sequence	Number of nucleotide substitutions
H574	9 to 12	11.4 (8 of 70)	6	CD25+FoxP3+Helios-	1	CD25+FoxP3+Helios+	16
				CD25+FoxP3+Helios+	1		
				CD25-FoxP3-Helios+	1		
				CD25-FoxP3-Helios-	1		
H605	27 to 30	6.8 (3 of 44)	39	CD25-Foxp3-Helios-	3	CD25+FoxP3+Helios+	32
6233K12	16 to 38	1.9 (1 of 53)	30	CD25-FoxP3-Helios+	2	CD25-FoxP3-Helios+	30
9440A11*	>38	2.6 (1 of 38)	46	CD25+Helios+	4	CD25+Helios+	76
8710U11	>38	0 (0 of 39)	57	CD25-FoxP3-Helios-	32	CD25-FoxP3-Helios-	67
8975T11	>54	0 (0 of 55)	53	CD25-FoxP3-Helios+	54	CD25-FoxP3-Helios-	86

We also analyzed plasma- and cell-derived EnvV1V3 amplicons from two HIV+ subjects (3806A11 and 9440A11) infected for more than 3.2 years using next generation sequencing to detect "rare" quasi-identical sequence pairs we might have missed in the previous analyses. Between 780 and 10000 EnvV1V3 sequences were first reconstructed using QuasiRecomb (51). The 50 most frequent sequences/population were aligned and sequences compared (S3 Fig). The closest cell-associated and plasma sequences were 6 and 14 nucleotide substitutions apart for 3806A11 and 9440A11, respectively, inconsistent with a major contribution of peripheral memory CD4+ T cell subsets to plasma virus production. Blast searching all plasma sequence variants against the 150 highest frequency cell-derived variants (per sorted cell subset) identified the closest pairs as 4 (3806A11, CD25-FoxP3-Helios+) and 10 (9440A11, CD25+Helios+) nucleotides apart.

Discussion

HIV plasma viremia predicts the rate of HIV disease progression (1,52) and depends on active HIV viral replication in CD4+ cells. Memory CD4 T cells are most probably the primary substrate for virus replication (11,53–55). HIV infection rates differ substantially between different CD4 T cell subsets (4–6,56). Recent data show that follicular T Helper (Tfh) cells are a prime target for virus replication and contribute to virion production even in elite controlling rhesus macaques (19) and most probably to plasma viremia (17). To what extent other CD4+ cell subsets contribute to plasma virus production in viremic progressors is unclear. In various *in vitro* infection models, HIV replication is associated with IL2 signaling and CD25 expression on stimulated CD4 T cells (10,n,14,21–23). Because IL2 is important for the homeostatic

proliferation of the CD25+FoxP3+ CD4 T cells (35,57), and because of high in vivo proliferation rates of this subset (32), we hypothesized that CD25+FoxP3+ CD4 T cells constitute a prime target for HIV infection and may contribute to plasma virion production in vivo.

Consistent with a previous report, we show that a large fraction of CD25+FoxP3+ CD4 T cells, express the HIV co-receptor CCR5 (35), potentially supporting viral entry. Although frequencies of CD25+FoxP3+ CD4 T cells were slightly elevated in viremic, HIV+ subjects, absolute cell numbers of this subset were significantly depleted, which confirms previously published data (41,43,59). A greater proportion of CD25+FoxP3+ memory CD4 T cells from HIV+ subjects expressed Ki67+ with almost one third of these cells "cycling" at any given time. This pattern – depleted cell counts despite increased fractions of Ki67+, "cycling" cells demonstrates that homeostasis of CD25+FoxP3+ CD4 T cells is heavily perturbed by HIV infection. Furthermore, expression of CCR5 and high proportions of cycling cells within CD25+FoxP3+ CD4 T cells should support both cell entry and reverse transcription of HIV, which is supported by the increased HIV DNA loads observed in memory CD25+FoxP3+ CD4 T cells observed in this study (m,36). Other reports show discrepant results regarding in vivo levels of HIV DNA in "regulatory" CD4 T cells - typically defined by $CD25^{high}$ phenotype, instead of the definition using co-expression of CD25 and FoxP3 that we used (58,60,61). Tran et al. observed a higher infection rate in $CD25^{high}$ than CD25 negative CD4 T cells (62), but did not exclude naïve CD4 T cells – which are not susceptible to CCR5-topic strains which predominate throughout most of the infection course. Of note, high in vivo proliferation of memory CD25+FoxP3+ CD4 T cells could also potentially pass on proviral HIV DNA to the cell progeny in the absence of productive HIV infection during ART. Previous studies reported that $CD25^{high}$ T cells (which were >99% FoxP3+) release virus upon in vitro restimulation and have ~3-fold

490 higher HIV infection rates compared to other CD4 T cells upon in vitro activation (36,62).
491 Together these data suggest that CD25+FoxP3+ CD4 T cells are a prime cellular target for HIV
492 infection that might serve as an important HIV reservoir during ART.

493 We next wanted to address whether memory CD25+FoxP3+ CD4 T cells could potentially
494 contribute to plasma virion production. Because cell fixation complicates analyses of HIV
495 transcription in sorted cell populations defined by intranuclear transcription factors (such as
496 FoxP3), we decided to study the phylogenetic relationship between plasma- and cell-derived
497 sequences within the highly variable EnvV1V3 region; if CD25+FoxP3+ memory CD4 T cells
498 significantly contribute to plasma virion production, EnvV1V3 DNA sequences derived from
499 this cell population should often be quasi-identical or preferentially cluster with plasma-derived
500 sequences. A previous study had reported rapid replacement of cell- and plasma-derived HIV
501 sequences by an incoming superinfecting HIV strain (63), implying a highly dynamic exchange
502 between these two compartments. In our study, detection of quasi-identical sequence pairs
503 derived from cells and plasma was rare and their fraction further decreased with infection
504 duration, which is consistent with the broadening of the viral reservoir with time. There was no
505 clear pattern of phylogenetic clustering of the plasma virus with any of the cell subset-derived
506 sequences we had sorted. In fact, cell-derived sequences did not "behave differently" from
507 plasma-derived sequences and sequences from both compartments intermingled. Our
508 phylogenetic data therefore do not allow definite conclusions about the cellular origin of plasma
509 virions. The high variability between individual plasma-derived sequences during chronic
510 infection emphasizes that a huge number of infected cells must contribute to plasma virion
511 production at any given time during chronic infection. It might hence be difficult to determine
512 the exact cellular origins of plasma virus through phylogenetic sequence analyses. Nonetheless,

513 in our analyses of individual sequences, we did find several quasi-identical sequence pairs
514 between plasma and CD25+FoxP3+ CD4 T cells, indicating that they may contribute to the
515 plasma viremia. One limitation of our study was that we used comparatively small amounts of
516 PBMC and plasma (compared to the total body amount) for phylogenetic analyses and we
517 therefore probably included insufficient numbers for detection of clusters of cell- and plasma-
518 derived sequences (76). Virus sequences from very large amounts of specimen will need to be
519 analyzed and optimally include material from secondary lymphoid tissues for more conclusive
520 answers. Secondary lymphoid tissues are thought to constitute the primary site for virion
521 production (reviewed in (63)). After ART interruption, onset of viral RNA transcription in lymph
522 nodes coincides with a rise in plasma viral load (73). CD25+FoxP3+ CD4 T cells in secondary
523 lymphoid organs contain high frequencies of Ki67+ "cycling" cells with significant capacity for
524 IL2 production and often express a CD69+ "recently activated" phenotype (74) and hence differ
525 from those in peripheral blood. A recent study detected colocalization of SIV_p27- and FoxP3
526 expression in intestinal tissues using confocal microscopy (75). We therefore consider it likely
527 that CD25+FoxP3+ CD4 T cells in lymphoid tissues are a targeted by HIV, but additional studies
528 will be needed to define the role of CD25+FoxP3+ CD4 T cells for plasma virion production in
529 vivo.

530

531 We also sorted memory CD4 T cell populations depending on their Helios expression. Helios
532 is an Ikaros transcriptional factor family member is critical for the regulatory function of
533 CD25+FoxP3+ CD4 T cells (46–48) and for the prevention of autoimmunity (49). Helios
534 modulates cell cycle progression and sustained cell survival through regulation of genes involved
535 in IL-2 signalling (49,50). Helios expression is also linked to expression of a range of

suppressive T cell markers and can be induced in CD4 T cells upon in vitro activation (64,65). In vitro, dividing CD25+FoxP3+CD4 T cells co-express Helios, while non-dividing regulatory T cells lose expression of FoxP3 and Helios, suggesting Helios as a marker of recently divided cells. In the same set of in vitro experiments, CD25-Helios+ CD4 T cells were composed of a highly activated "effector" memory cells (64). We detected higher median Gag DNA loads in memory CD25+FoxP3+ in both Helios positive (26-fold increased) and negative (119-fold increased) as well as CD25-FoxP3- Helios+ memory CD4 T cells (104-fold increased) compared to FoxP3-CD25- Helios- memory CD4 T cells. It is remarkable that we often did not detect HIV-DNA in this "dominant" memory CD4 T cell subset. A history of more frequent or recent cell divisions within CD25-FoxP3- Helios+ memory CD4 T cells might have contributed to high HIV susceptibility in this memory subset, whereas removal of such cells in the sorted CD25-FoxP3-Helios- memory CD4 T cells, could potentially explain the low HIV infection rates observed in this memory cell subset. "Non-activated", circulating memory CD4 T cells are probably less susceptible and accumulate less HIV DNA over time, in comparison to other memory CD4 T cell subsets with a history of in vivo proliferation. Helios deficient regulatory CD4 T cells exhibit an activated phenotype, increased capacity to secrete IFNγ and develop into non-anergic cells under inflammatory conditions (49,66). Increased responsiveness to cellular activation in comparison to their Helios+ counterparts signalling could potentially explain the higher HIV-DNA levels in CD25+FoxP3+ Helios- memory CD4 T cells compared to their Helios+ counterparts. These data show that Helios and CD25/FoxP3 expression patterns are linked to different cellular HIV infection rates, consistent with a role of the IL2 signalling pathway for HIV infection in vivo.

In conclusion, we find that homeostasis of CD25+FoxP3+ CD4 T cells is heavily perturbed during HIV infection. High expression of HIV coreceptor-CCR5 and in vivo proliferation potentially facilitates efficient HIV infection of memory CD25+FoxP3+ CD4 T cells. Furthermore, high proliferative activity of this cell subset is likely to passage of HIV DNA to cell progeny in the absence of active viral replication. This subset could therefore serve as an important viral reservoir during ART. Neither circulating memory CD25+FoxP3+ CD4 T cell- nor any of the other memory CD4 T cell subset-derived EnvV1V3 sequences preferentially clustered with plasma-derived sequences. Instead, sequences from the two compartments intermingled and the genetic distance in-between and within the two compartments increased with infection duration, precluding definite conclusion about the cellular origin of the plasma virus in this study.

Acknowledgements

We would like to thank Brenna Hill from the Vaccine Research Center, NIH in Bethesda for providing HIV_Gag DNA standard and Andreas Wieser from the Max von Pettenkofer Institute, Medical Center of the University of Munich (LMU) for advice to include a PCR error control. The following reagent was obtained through the NIH AIDS Reagent Program, Division of AIDS, NIAID, NIH from Drs. D. Montefiori, F. Gao, C. Williamson and S. Abdool Karim: Du422, clone 1 (SVPC5).

Funding information

The WHIS study was funded by the German Research Foundation (DFG, grant SA 1878/1-1) with additional support by the European Community's Seventh Framework Programme (FP7/2007–2013 and FP7/ 2007–2011 under EC-GA nu 241642) and by the German Center for Infection Research (DZIF) while the HHECO study was supported by the German Federal Ministry of Education and Research to Dr. Feldt (EDCTP Project 01KA1102). Deep sequencing was supported by Transvac European Network and funded under the European Comission`s 7th Framework Programe (FP7). The funders had no role in study design, data collection and analysis, preparation of the manuscript or decision to submit the work for publication.

589 # References

590 1. Mellors JW, Rinaldo CR, Gupta P, White RM, Todd JA, Kingsley LA. Prognosis in HIV-
591 1 infection predicted by the quantity of virus in plasma. Science (80). 1996 May
592 24;272(5265):1167–70.

593 2. Li TS, Tubiana R, Katlama C, Calvez V, Ait Mohand H, Autran B. Long-lasting recovery
594 in CD4 T-cell function and viral-load reduction after highly active antiretroviral therapy in
595 advanced HIV-1 disease. Lancet. 1998 Jun 6;351(9117):1682–6.

596 3. Verhofstede C, Reniers S, Van Wanzeele F, Plum J. Evaluation of proviral copy number
597 and plasma RNA level as early indicators of progression in HIV-1 infection: correlation
598 with virological and immunological markers of disease. AIDS. 1994 Oct;8(10):1421–7.

599 4. Ganesan A, Chattopadhyay PK, Brodie TM, Qin J, Mascola JR, Michael NL, et al.
600 Immunological and Virological Events in Early HIV Infection Predict Subsequent Rate of
601 Progression. J Infect Dis. 2010;201(2):272–84.

602 5. Brenchley JM, Schacker TW, Ruff LE, Price DA, Taylor JH, Beilman GJ, et al. CD4+ T
603 cell depletion during all stages of HIV disease occurs predominantly in the gastrointestinal
604 tract. J Exp Med. 2004 Sep 20;200(6):749–59.

605 6. Chomont N, El-Far M, Ancuta P, Trautmann L, Procopio F a, Yassine-Diab B, et al. HIV
606 reservoir size and persistence are driven by T cell survival and homeostatic proliferation.
607 Nat Med. 2009 Aug;15(8):893–900.

608 7. Casazza JP, Brenchley JM, Hill BJ, Ayana R, Ambrozak D, Roederer M, et al. Autocrine
609 production of beta-chemokines protects CMV-Specific CD4 T cells from HIV infection.
610 PLoS Pathog. 2009 Oct;5(10):e1000646.

611 8. Douek DC, Brenchley JM, Betts MR, Ambrozak DR, Hill BJ, Okamoto Y, et al. HIV
612 preferentially infects HIV-specific CD4+ T cells. Nature. 2002 May 2;417(6884):95–8.
613 9. Geldmacher C, Koup RA. Pathogen-specific T cell depletion and reactivation of
614 opportunistic pathogens in HIV infection. Trends Immunol. 20m May;33(5):207–14.
615 10. Geldmacher C, Ngwenyama N, Schuetz A, Petrovas C, Reither K, Heeregrave EJ, et al.
616 Preferential infection and depletion of Mycobacterium tuberculosis-specific CD4 T cells
617 after HIV-1 infection. J Exp Med. 2010 Dec 20;207(n):2869–81.
618 11. Zhang Z, Schuler T, Zupancic M, Wietgrefe S, Staskus KA, Reimann KA, et al. Sexual
619 transmission and propagation of SIV and HIV in resting and activated CD4+ T cells.
620 Science. 1999 Nov m;286(5443):n53–7.
621 m. Zack JA, Arrigo SJ, Weitsman SR, Go AS, Haislip A, Chen IS. HIV-1 entry into
622 quiescent primary lymphocytes: molecular analysis reveals a labile, latent viral structure.
623 Cell. 1990 Apr 20;61(2):2n–22.
624 n. Chou CS, Ramilo O, Vitetta ES. Highly purified CD25- resting T cells cannot be infected
625 de novo with HIV-1. Proc Natl Acad Sci U S A. 1997 Feb 18;94(4):n61–5.
626 14. Biancotto A, Iglehart SJ, Vanpouille C, Condack CE, Lisco A, Ruecker E, et al. HIV-1
627 induced activation of CD4+ T cells creates new targets for HIV-1 infection in human
628 lymphoid tissue ex vivo. Blood. 2008 Jan 15;111(2):699–704.
629 15. Maenetje P, Riou C, Casazza JP, Ambrozak D, Hill B, Gray G, et al. A steady state of
630 CD4+ T cell memory maturation and activation is established during primary subtype C
631 HIV-1 infection. J Immunol. 2010 May 1;184(9):4926–35.
632 16. Crotty S. T Follicular Helper Cell Differentiation, Function, and Roles in Disease.

633 Immunity. 2014 Oct 16;41(4):529–42.

634 17. Perreau M, Savoye A-L, De Crignis E, Corpataux J-M, Cubas R, Haddad EK, et al.
635 Follicular helper T cells serve as the major CD4 T cell compartment for HIV-1 infection,
636 replication, and production. J Exp Med. 20n Jan 14;210(1):143–56.

637 18. Pallikkuth S, Sharkey M, Babic DZ, Gupta S, Stone GW, Fischl MA, et al. Peripheral T
638 Follicular Helper Cells Are the Major HIV Reservoir Within Central Memory CD4 T
639 Cells in Peripheral Blood from chronic HIV infected individuals on cART. J Virol. 2015
640 Dec 16;JVI.02883–15.

641 19. Fukazawa Y, Lum R, Okoye AA, Park H, Matsuda K, Bae JY, et al. B cell follicle
642 sanctuary permits persistent productive simian immunodeficiency virus infection in elite
643 controllers. Nat Med. 2015 Feb 1;21(2):n2–9.

644 20. Boyman O, Sprent J. The role of interleukin-2 during homeostasis and activation of the
645 immune system. Nat Rev Immunol. 20m Mar;m(3):180–90.

646 21. Finberg RW, Wahl SM, Allen JB, Soman G, Strom TB, Murphy JR, et al. Selective
647 elimination of HIV-1-infected cells with an interleukin-2 receptor-specific cytotoxin.
648 Science. 1991 Jun 21;252(50n):1703–5.

649 22. Ramilo O, Bell KD, Uhr JW, Vitetta ES. Role of CD25+ and CD25-T cells in acute HIV
650 infection in vitro. J Immunol. 1993 Jun 1;150(11):5202–8.

651 23. Goletti D, Weissman D, Jackson RW, Graham NM, Vlahov D, Klein RS, et al. Effect of
652 Mycobacterium tuberculosis on HIV replication. Role of immune activation. J Immunol.
653 1996 Aug 1;157(3):m71–8.

654 24. Baecher-Allan C, Brown JA, Freeman GJ, Hafler DA. CD4+CD25+ regulatory cells from

655 human peripheral blood express very high levels of CD25 ex vivo. Novartis Found Symp.
656 2003 Jan;252:67–91, 106–14.

657 25. Seddiki N, Santner-Nanan B, Martinson J, Zaunders J, Sasson S, Landay A, et al.
658 Expression of interleukin (IL)-2 and IL-7 receptors discriminates between human
659 regulatory and activated T cells. J Exp Med. 2006 Jul 10;203(7):1693–700.

660 26. Hori S, Takahashi T, Sakaguchi S. Control of autoimmunity by naturally arising
661 regulatory CD4+ T cells. Adv Immunol. 2003 Jan;81:331–71.

662 27. Sakaguchi S, Yamaguchi T, Nomura T, Ono M. Regulatory T cells and immune tolerance.
663 Cell. 2008 May 30;n3(5):775–87.

664 28. Aandahl EM, Michaëlsson J, Moretto WJ, Hecht FM, Nixon DF. Human CD4+ CD25+
665 regulatory T cells control T-cell responses to human immunodeficiency virus and
666 cytomegalovirus antigens. J Virol. 2004 Mar;78(5):2454–9.

667 29. Kinter AL, Horak R, Sion M, Riggin L, McNally J, Lin Y, et al. CD25+ regulatory T cells
668 isolated from HIV-infected individuals suppress the cytolytic and nonlytic antiviral
669 activity of HIV-specific CD8+ T cells in vitro. AIDS Res Hum Retroviruses. 2007
670 Mar;23(3):438–50.

671 30. Booth NJ, McQuaid AJ, Sobande T, Kissane S, Agius E, Jackson SE, et al. Different
672 proliferative potential and migratory characteristics of human CD4+ regulatory T cells
673 that express either CD45RA or CD45RO. J Immunol. 2010 Apr 15;184(8):4317–26.

674 31. Antons AK, Wang R, Oswald-Richter K, Tseng M, Arendt CW, Kalams SA, et al. Naive
675 precursors of human regulatory T cells require FoxP3 for suppression and are susceptible
676 to HIV infection. J Immunol. 2008 Jan 15;180(2):764–73.

677 32. Peters JH, Koenen HJPM, Fasse E, Tijssen HJ, Ijzermans JNM, Groenen PJTA, et al.
678 Human secondary lymphoid organs typically contain polyclonally-activated proliferating
679 regulatory T cells. Blood. American Society of Hematology; 20n Sep 26;m2(n):22n–23.
680 33. Vukmanovic-stejic M, Zhang Y, Cook JE, Fletcher JM, Mcquaid A, Masters JE, et al.
681 Human CD4+CD25hiFoxp3+ regulatory T cells are derived by rapid turnover of memory
682 populations in vivo. J Clin Invest. 2006;116(9):2423–33.
683 34. Vukmanovic-Stejic M, Agius E, Booth N, Dunne PJ, Lacy KE, Reed JR, et al. The
684 kinetics of CD4+Foxp3+ T cell accumulation during a human cutaneous antigen-specific
685 memory response in vivo. J Clin Invest. 2008 Nov 3;118(11):3639–50.
686 35. Sakaguchi S, Ono M, Setoguchi R, Yagi H, Hori S, Fehervari Z, et al. Foxp3+ CD25+
687 CD4+ natural regulatory T cells in dominant self-tolerance and autoimmune disease.
688 Immunol Rev. 2006 Aug;2m:8–27.
689 36. Oswald-Richter K, Grill SM, Shariat N, Leelawong M, Sundrud MS, Haas DW, et al. HIV
690 infection of naturally occurring and genetically reprogrammed human regulatory T-cells.
691 PLoS Biol. 2004 Jul 1;2(7):E198.
692 37. Chachage M, Podola L, Clowes P, Nsojo A, Bauer A, Mgaya O, et al. Helminth-
693 associated systemic immune activation and HIV co-receptor expression: Response to
694 Albendazole/Praziquantel treatment. PLoS Negl Trop Dis. 2014 Mar;8(3):e2755.
695 38. Sarfo FS, Eberhardt KA, Dompreh A, Kuffour EO, Soltau M, Schachscheider M, et al.
696 Helicobacter pylori Infection Is Associated with Higher CD4 T Cell Counts and Lower
697 HIV-1 Viral Loads in ART-Naïve HIV-Positive Patients in Ghana. PLoS One.
698 2015;10(11):e0143388.

699 39. Eberhardt K a, Sarfo FS, Dompreh a, Kuffour EO, Geldmacher C, Soltau M, et al.
700 Helicobacter pylori Coinfection Is Associated with Decreased Markers of Immune
701 Activation in ART-Naive HIV-Positive and in HIV-Negative Individuals in Ghana. Clin
702 Infect Dis. 2015;61(10):1615–23.

703 40. Geldmacher C, Currier JR, Herrmann E, Haule A, Kuta E, McCutchan F, et al. CD8 T-cell
704 recognition of multiple epitopes within specific Gag regions is associated with
705 maintenance of a low steady-state viremia in human immunodeficiency virus type 1-
706 seropositive patients. J Virol. 2007 Mar;81(5):2440–8.

707 41. Angin M, Kwon DS, Streeck H, Wen F, King M, Rezai A, et al. Preserved function of
708 regulatory T cells in chronic HIV-1 infection despite decreased numbers in blood and
709 tissue. J Infect Dis. 20m May 15;205(10):1495–500.

710 42. Schulze Zur Wiesch J, Thomssen A, Hartjen P, Tóth I, Lehmann C, Meyer-Olson D, et al.
711 Comprehensive analysis of frequency and phenotype of T regulatory cells in HIV
712 infection: CD39 expression of FoxP3+ T regulatory cells correlates with progressive
713 disease. J Virol. 2011 Feb 1;85(3):m87–97.

714 43. Presicce P, Orsborn K, King E, Pratt J, Fichtenbaum CJ, Chougnet CA. Frequency of
715 circulating regulatory T cells increases during chronic HIV infection and is largely
716 controlled by highly active antiretroviral therapy. PLoS One. 2011 Jan 5;6(m):e28118.

717 44. Montes M, Lewis DE, Sanchez C, Lopez de Castilla D, Graviss EA, Seas C, et al. Foxp3+
718 regulatory T cells in antiretroviral-naive HIV patients. AIDS. 2006 Aug 1;20(m):1669–71.

719 45. Simonetta F, Lecuroux C, Girault I, Goujard C, Sinet M, Lambotte O, et al. Early and
720 long-lasting alteration of effector CD45RA(-)Foxp3(high) regulatory T-cell homeostasis

during HIV infection. J Infect Dis. 20m May 15;205(10):1510–9.

46. Sugimoto N, Oida T, Hirota K, Nakamura K, Nomura T, Uchiyama T, et al. Foxp3-dependent and -independent molecules specific for CD25+CD4+ natural regulatory T cells revealed by DNA microarray analysis. Int Immunol. 2006 Aug 1;18(8):1197–209.

47. Thornton AM, Korty PE, Tran DQ, Wohlfert E a, Murray PE, Belkaid Y, et al. Expression of Helios, an Ikaros transcription factor family member, differentiates thymic-derived from peripherally induced Foxp3+ T regulatory cells. J Immunol. 2010 Apr 1;184(7):3433–41.

48. Getnet D, Grosso JF, Goldberg M V, Harris TJ, Yen H-R, Bruno TC, et al. A role for the transcription factor Helios in human CD4(+)CD25(+) regulatory T cells. Mol Immunol. 2010 Apr;47(7-8):1595–600.

49. Kim H-J, Barnitz RA, Kreslavsky T, Brown FD, Moffett H, Lemieux ME, et al. Stable inhibitory activity of regulatory T cells requires the transcription factor Helios. Science (80). 2015 Oct 15;350(6258):334–9.

50. Baine I, Basu S, Ames R, Sellers RS, Macian F. Helios Induces Epigenetic Silencing of Il2 Gene Expression in Regulatory T Cells. J Immunol. 20m Dec 28;190(3):1008–16.

51. Töpfer A, Zagordi O, Prabhakaran S, Roth V, Halperin E, Beerenwinkel N. Probabilistic inference of viral quasispecies subject to recombination. J Comput Biol. 20n Feb;20(2):1n–23.

52. Ioannidis JP, Cappelleri JC, Lau J, Sacks HS, Skolnik PR. Predictive value of viral load measurements in asymptomatic untreated HIV-1 infection: a mathematical model. AIDS. 1996 Mar;10(3):255–62.

743 53. Haase AT. Population biology of HIV-1 infection: viral and CD4+ T cell demographics
744 and dynamics in lymphatic tissues. Annu Rev Immunol. 1999 Jan;17:625–56.
745 54. Veazey RS, DeMaria M, Chalifoux L V, Shvetz DE, Pauley DR, Knight HL, et al.
746 Gastrointestinal tract as a major site of CD4+ T cell depletion and viral replication in SIV
747 infection. Science. 1998 Apr 17;280(5362):427–31.
748 55. Schacker T, Little S, Connick E, Gebhard K, Zhang ZQ, Krieger J, et al. Productive
749 infection of T cells in lymphoid tissues during primary and early human
750 immunodeficiency virus infection. J Infect Dis. 2001 Mar 15;183(4):555–62.
751 56. Brenchley JM, Hill BJ, Ambrozak DR, Price DA, Guenaga FJ, Casazza JP, et al. T-cell
752 subsets that harbor human immunodeficiency virus (HIV) in vivo: implications for HIV
753 pathogenesis. J Virol. 2004 Feb;78(3):1160–8.
754 57. Setoguchi R, Hori S, Takahashi T, Sakaguchi S. Homeostatic maintenance of natural
755 Foxp3(+) CD25(+) CD4(+) regulatory T cells by interleukin (IL)-2 and induction of
756 autoimmune disease by IL-2 neutralization. J Exp Med. 2005 Mar 7;201(5):723–35.
757 58. Moreno-Fernandez ME, Zapata W, Blackard JT, Franchini G, Chougnet CA. Human
758 regulatory T cells are targets for human immunodeficiency Virus (HIV) infection, and
759 their susceptibility differs depending on the HIV type 1 strain. J Virol. 2009
760 Dec;83(24):m925–33.
761 59. Nilsson J, Boasso A, Velilla PA, Zhang R, Vaccari M, Franchini G, et al. HIV-1-driven
762 regulatory T-cell accumulation in lymphoid tissues is associated with disease progression
763 in HIV/AIDS. Blood. 2006 Dec 1;108(m):3808–17.
764 60. Dunham RM, Cervasi B, Brenchley JM, Albrecht H, Weintrob A, Sumpter B, et al. CDm7

765 and CD25 Expression Defines CD4+ T Cell Subsets That Are Differentially Depleted
766 during HIV Infection. J Immunol. 2008;180(8):5582–92.

767 61. Chase AJ, Yang H-C, Zhang H, Blankson JN, Siliciano RF. Preservation of FoxP3+
768 regulatory T cells in the peripheral blood of human immunodeficiency virus type 1-
769 infected elite suppressors correlates with low CD4+ T-cell activation. J Virol. 2008
770 Sep;82(17):8307–15.

771 62. Tran T-A, de Goër de Herve M-G, Hendel-Chavez H, Dembele B, Le Névot E, Abbed K,
772 et al. Resting regulatory CD4 T cells: a site of HIV persistence in patients on long-term
773 effective antiretroviral therapy. PLoS One. 2008 Jan;3(10):e3305.

774 63. McCutchan FE, Hoelscher M, Tovanabutra S, Piyasirisilp S, Sanders-Buell E, Ramos G,
775 et al. In-depth analysis of a heterosexually acquired human immunodeficiency virus type 1
776 superinfection: evolution, temporal fluctuation, and intercompartment dynamics from the
777 seronegative window period through 30 months postinfection. J Virol. 2005 Sep
778 1;79(18):11693–704.

779 64. Akimova T, Beier UH, Wang L, Levine MH, Hancock WW. Helios expression is a
780 marker of T cell activation and proliferation. PLoS One. 2011 Jan;6(8):e24226.

781 65. Verhagen J, Wraith DC. Comment on "Expression of Helios, an Ikaros transcription factor
782 family member, differentiates thymic-derived from peripherally induced Foxp3+ T
783 regulatory cells". J Immunol. 2010 Dec 15;185(m):7m9.

784 66. Sebastian M, Lopez-Ocasio M, Metidji A, Rieder SA, Shevach EM, Thornton AM. Helios
785 Controls a Limited Subset of Regulatory T Cell Functions. J Immunol. 2015 Nov
786 18;196(1):144–55.

787 67. Hoffmann D, Wolfarth B, Hörterer HG, Halle M, Reichhuber C, Nadas K, et al. Elevated
788 Epstein-Barr virus loads and lower antibody titers in competitive athletes. J Med Virol.
789 2010 Mar;82(3):446–51.
790 68. Li M, Salazar-Gonzalez JF, Derdeyn CA, Morris L, Williamson C, Robinson JE, et al.
791 Genetic and neutralization properties of subtype C human immunodeficiency virus type 1
792 molecular env clones from acute and early heterosexually acquired infections in Southern
793 Africa. J Virol. 2006 Dec;80(23):11776–90.
794 69. Pollakis G, Baan E, van Werkhoven MB, Berkhout B, Bakker M, Jurriaans S, et al.
795 Association between gpm0 envelope V1V2 and V4V5 variable loop profiles in a defined
796 HIV-1 transmission cluster. AIDS. 2015 Jun 19;29(10):1161–71.
797 70. Tamura K, Stecher G, Peterson D, Filipski A, Kumar S. MEGA6: Molecular Evolutionary
798 Genetics Analysis version 6.0. Mol Biol Evol. 20n Dec;30(m):2725–9.
799 71. Nei M, Kumar S. Molecular Evolution and Phylogenetics. Oxford University Press; 2000.
800 352 p.
801 72. Benson DA, Karsch-Mizrachi I, Lipman DJ, Ostell J, Sayers EW. GenBank. Nucleic
802 Acids Res. 2009 Jan;37(Database issue):D26–31.
803 73. Hoffmann S, Otto C, Kurtz S, Sharma CM, Khaitovich P, Vogel J, et al. Fast mapping of
804 short sequences with mismatches, insertions and deletions using index structures. PLoS
805 Comput Biol. 2009 Sep;5(9):e1000502.
806 74. Li H, Handsaker B, Wysoker A, Fennell T, Ruan J, Homer N, et al. The Sequence
807 Alignment/Map format and SAMtools. Bioinformatics. 2009 Aug 15;25(16):2078–9.
808 75. Kimura M. A simple method for estimating evolutionary rates of base substitutions

809 through comparative studies of nucleotide sequences. J Mol Evol. 1980 Dec;16(2):111–
810 20.

811

812

Figure Legends

Fig 1. Frequencies and absolute numbers of CD25+ FoxP3+ regulatory T cells in the peripheral blood in relation to HIV infection. Representative dot plots and gating strategy for the detection of regulatory T cells through CD25 and FoxP3 expression on $CD3^{+}CD4^{+}$ T cells are shown in (**A**). Regulatory CD4 T cell frequencies and absolute numbers were compared between HIV- and HIV+ subjects in (B) and (C), respectively. A correlation analysis of absolute CD4 counts and regulatory CD4 T cell counts is shown in (D). Statistical analysis was performed using Mann-Whitney test when comparing groups and Spearman r statistical test for correlation analyses.

Fig 2. Ex vivo HIV-co receptor (CCR5) expression on regulatory T cells. Shown is (**A**) a histogram overlay for CCR5 expression on total CD4 T cells (grey) and CD25+ Foxp3+ CD4 T cells (black). The frequencies of CCR5+ expressing Tregs are compared between HIV negative and positive subjects in (**B**). For maximum staining sensitivity, fresh anticoagulated whole blood was used to determine CCR5 expression on CD4 T cells. Statistical analysis was performed using Mann-Whitney test.

Fig 3. Ki67 expression in memory CD4 T cells and CD25+FoxP3+ Tregs in relation to HIV infection. Memory status of CD4 T cells was determined by CD45RA staining. The frequencies of Ki67+ cells are shown for memory CD25+FoxP3+ Tregs **(A)** and CD25-FoxP3- memory CD4 T cells (**B**) in relation to HIV infection status. A correlation analysis of Ki67 positive cells among memory CD25+FoxP3+ Tregs(Y axis) and CD25-FoxP3- memory CD4 T cells (X axis) is shown in (**C**) and includes HIV+ and HIV- subjects. A correlation analysis of the frequency of Ki67+ memory CD4 T cells and memory Tregs (**E**) versus CD4 T cell frequencies (% of CD3) in

HIV+ subjects is shown in (**D**) and (**E**) respectively. Statistical analysis was performed using Mann-Whitney test when comparing groups and Spearman r statistical test for correlation analyses.

Fig 4. Quantification of Cell associated HIV gag DNA in sorted memory CD4 T cell subsets. Gating/sorting strategy used to sort different memory CD4 T cell populations delineated by Helios, CD25 and FoxP3 expression (**A**). The number of gag copies/10^6cells detected in $CD25^-$ /$FoxP3^-$ and $CD25^+$/$FoxP3^+$ memory CD4 T cells from 21 different subjects is shown in (**B**). The number of gag copies/10^6cells detected in these memory CD4 T cell subsets further delineated by Helios expression is shown in (**C**). Gag DNA within different CD4 T cell populations of the same subject was quantified during the same RT-PCR run. The statistical analysis was performed using the Wilcoxon-rank-matched pairs test.

Fig 5. Phylogenetic relationship of HIV Envelope sequences derived from plasma and sorted memory CD4 T cell populations. Plasma- and cell-derived sequences of the highly variable EnvV1V3 region (Hxb 6559–7320) were amplified cloned, sequenced (n=384, Sanger method) and analyzed for 6 viremic subjects with differing HIV infection duration**.** The phylogenetic relationship was inferred by the Maximum Likelihood method based on the General Time Reversible substitution model (GTR+G, **A and B**). Correlation between frequency of cell-derived sequences that were quasi-identical to plasma-derived sequences and the estimated infection duration is shown in (**C**). P and r-values were calculated with the Pearson two-tailed statistical test.

Supporting Information

S1 Fig: Representative gating tree for analyses of Ki67 expression in memory CD4 T cell populations delineated by CD25 and FoxP3 expression in the HHECO cohort

S2 Fig: Plasma- and cell-derived EnvV1V3 nucleotide sequence variability increases with HIV infection duration within and between these compartments.

Linear regression analysis (green line) was performed using the Prism/GraphPad software package and P values were calculated with the Pearson two-tailed statistical test. The red line shows a second order polynomial regression analysis indicating that nucleotide variation may be reaching a plateau. A) Distance of the EnvV1V3 sequences derived from plasma to the sequences extracted from the corresponding cellular fractions plotted against the estimated duration of infection. B) Plasma sequences diversity plotted against the estimated duration of infection. The red line indicates a non-linear analysis performed using a second order polynomial equation taking into account the best-fit values. The evolutionary distances were computed using the Kimura 2-parameter method (75) and are in the units of the number of base substitutions per site including both Transitions + Transversions. The rate variation among sites was modelled with a gamma distribution. The analysis was conducted in MEGA6 (70). No sequence diversity was observed in the 8710 plasma fraction and thus was not included in the linear regression analysis with the P value been not significant if 8710 had been included.

S3 Fig: Phylogenetic analyses of HIV Envelope sequences derived from plasma and sorted memory CD4 T cell populations using a using Next Generation sequencing.

Shown is the phylogenetic analyses of EnvV1V3 sequences from the 50 most frequently detected sequences derived from either plasma or the different sorted memory CD4 T cell subsets for two viremic subjects of the WHIS cohort. The phylogenetic relationship was inferred by the Maximum Likelihood method based on the General Time Reversible substitution model (GTR+G). EnvV1V3 amplicons were directly subjected to next generation sequencing. Quasi-species reconstruction was performed using the software QuasiRecomb. The applied methods are described in detail in the material and methods section.

Figures

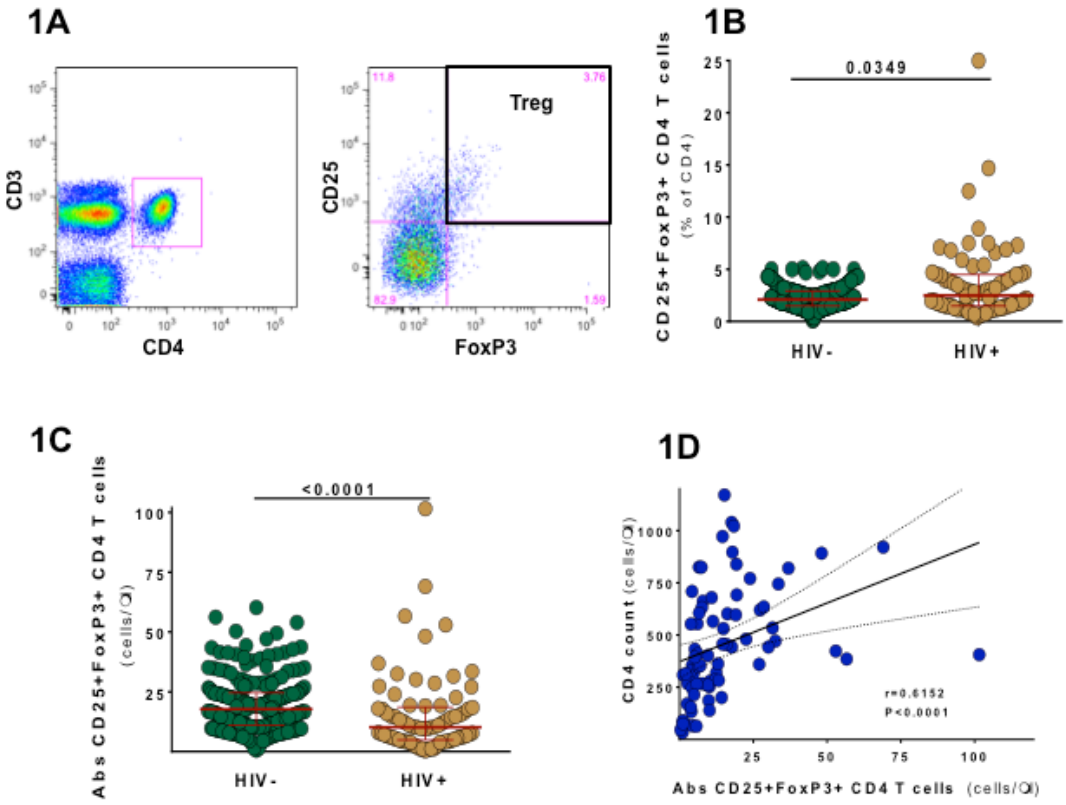

Fig 1. Frequencies and absolute numbers of CD25+ FoxP3+ regulatory T cells in the peripheral blood in relation to HIV infection. Representative dot plots and gating strategy for the detection of regulatory T cells through CD25 and FoxP3 expression on $CD3^{+}CD4^{+}$ T cells are shown in (**A**). Regulatory CD4 T cell frequencies and absolute numbers were compared between HIV- and HIV+ subjects in (B) and (C), respectively. A correlation analysis of absolute CD4 counts and regulatory CD4 T cell counts is shown in (D). Statistical analysis was performed using Mann-Whitney test when comparing groups and Spearman r statistical test for correlation analyses.

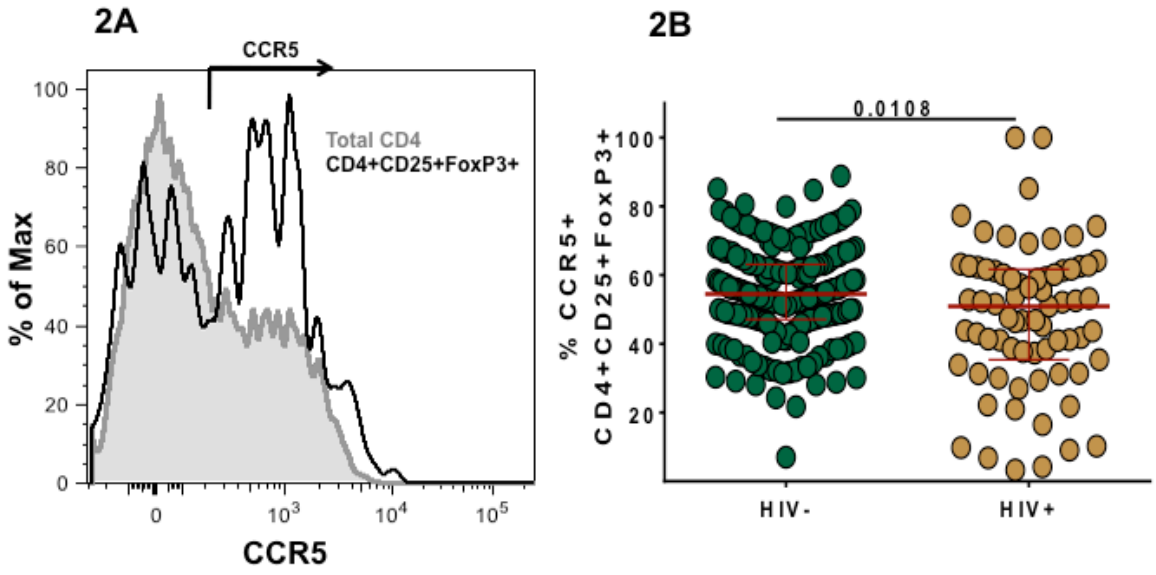

11

12 **Fig 2. Ex vivo HIV-co receptor (CCR5) expression on regulatory T cells**. Shown is (**A**) a
13 histogram overlay for CCR5 expression on total CD4 T cells (grey) and CD25+ Foxp3+ CD4 T
14 cells (black). The frequencies of CCR5+ expressing Tregs are compared between HIV negative
15 and positive subjects in (**B**). For maximum staining sensitivity, fresh anticoagulated whole blood
16 was used to determine CCR5 expression on CD4 T cells. Statistical analysis was performed
17 using Mann-Whitney test.

18

Figure 3

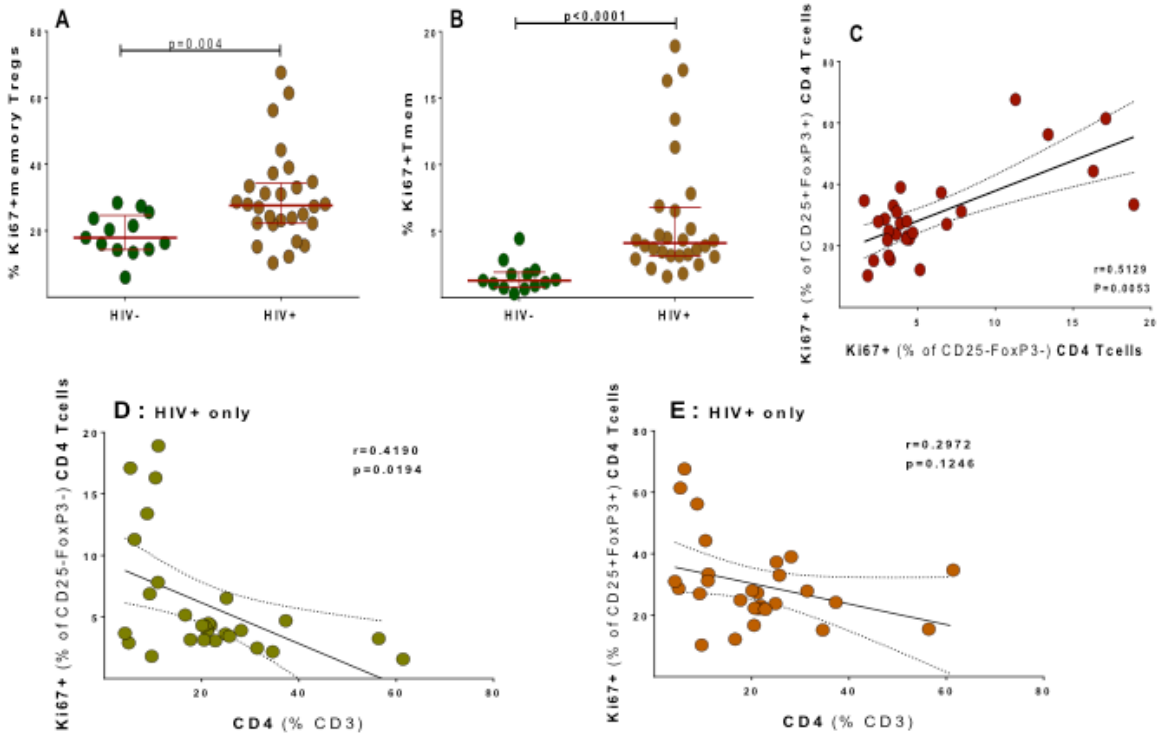

Fig 3. Ki67 expression in memory CD4 T cells and CD25+FoxP3+ Tregs in relation to HIV infection. Memory status of CD4 T cells was determined by CD45RA staining. The frequencies of Ki67+ cells are shown for memory CD25+FoxP3+ Tregs **(A)** and CD25-FoxP3- memory CD4 T cells (**B**) in relation to HIV infection status. A correlation analysis of Ki67 positive cells among memory CD25+FoxP3+ Tregs(Y axis) and CD25-FoxP3- memory CD4 T cells (X axis) is shown in (**C**) and includes HIV+ and HIV- subjects. A correlation analysis of the frequency of Ki67+ memory CD4 T cells and memory Tregs (**E**) versus CD4 T cell frequencies (% of CD3) in HIV+ subjects is shown in (**D**) and (**E**) respectively. Statistical analysis was performed using Mann-Whitney test when comparing groups and Spearman r statistical test for correlation analyses.

4A

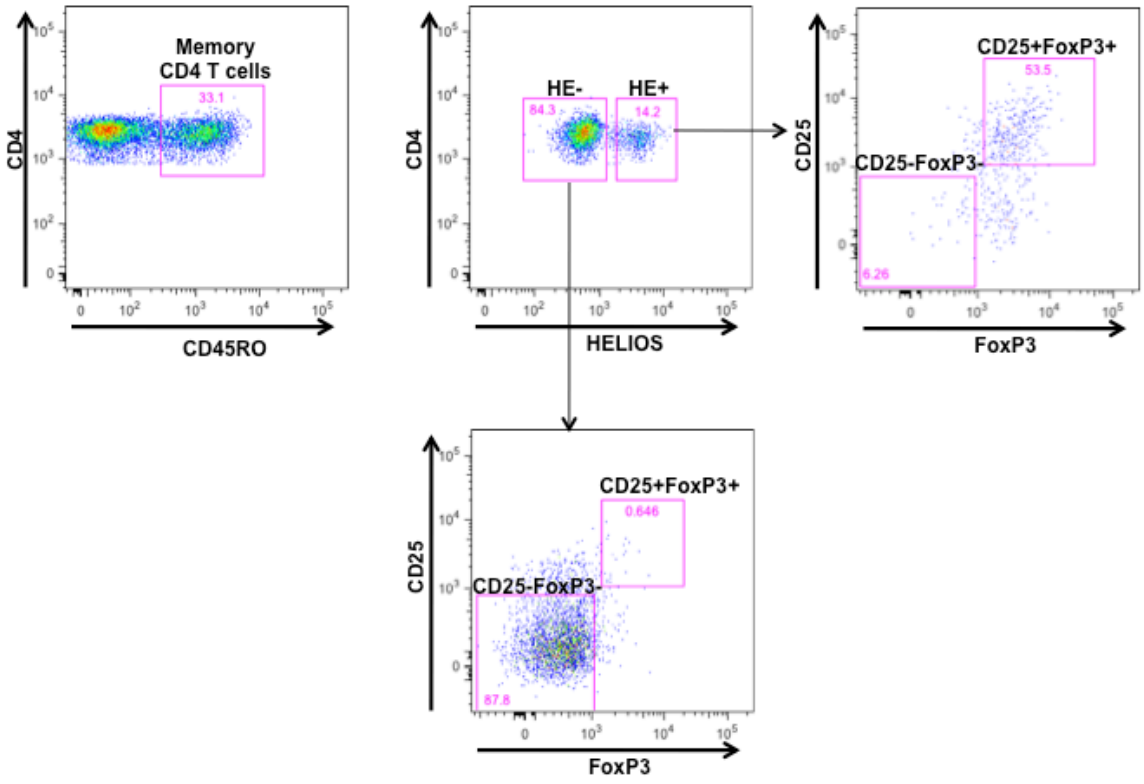
Memory
CD4 T cells
33.1
CD4
CD45RO
HE-
HE+
84.3
14.2
HELIOS
CD25+FoxP3+
53.5
CD25-FoxP3-
6.26
CD25
FoxP3
CD25+FoxP3+
0.646
CD25-FoxP3-
87.8
CD25
FoxP3

30

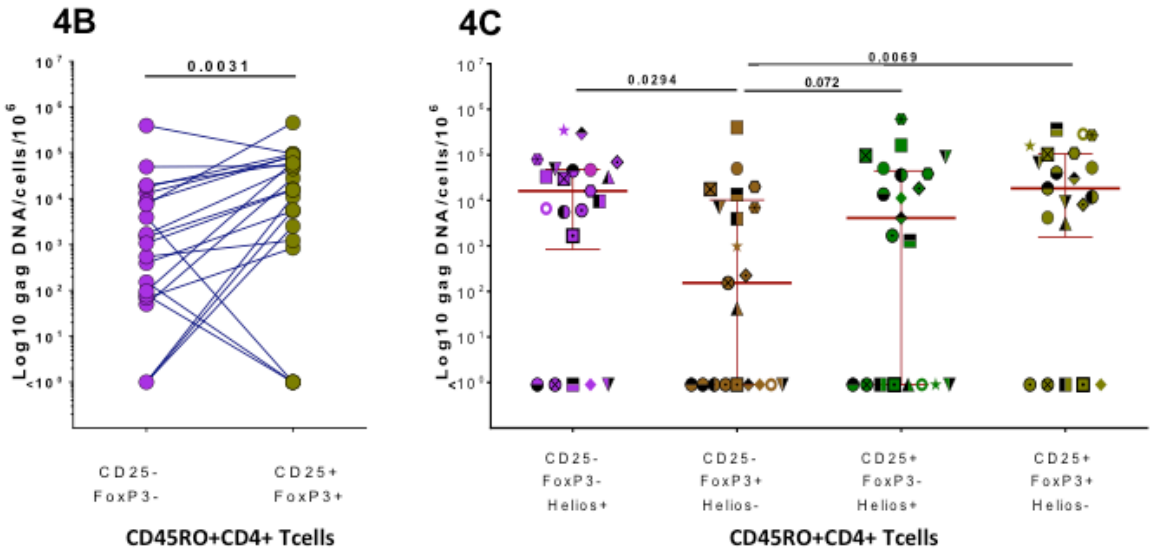

Fig 4. Quantification of Cell associated HIV gag DNA in sorted memory CD4 T cell subsets. Gating/sorting strategy used to sort different memory CD4 T cell populations delineated by Helios, CD25 and FoxP3 expression (**A**). The number of gag copies/10^6cells detected in $CD25^-$ /$FoxP3^-$ and $CD25^+$/$FoxP3^+$ memory CD4 T cells from 21 different subjects is shown in (**B**). The number of gag copies/10^6cells detected in these memory CD4 T cell subsets further delineated by Helios expression is shown in (**C**). Gag DNA within different CD4 T cell populations of the same subject was quantified during the same RT-PCR run. The statistical analysis was performed using the Wilcoxon-rank-matched pairs test.

Figure 5A

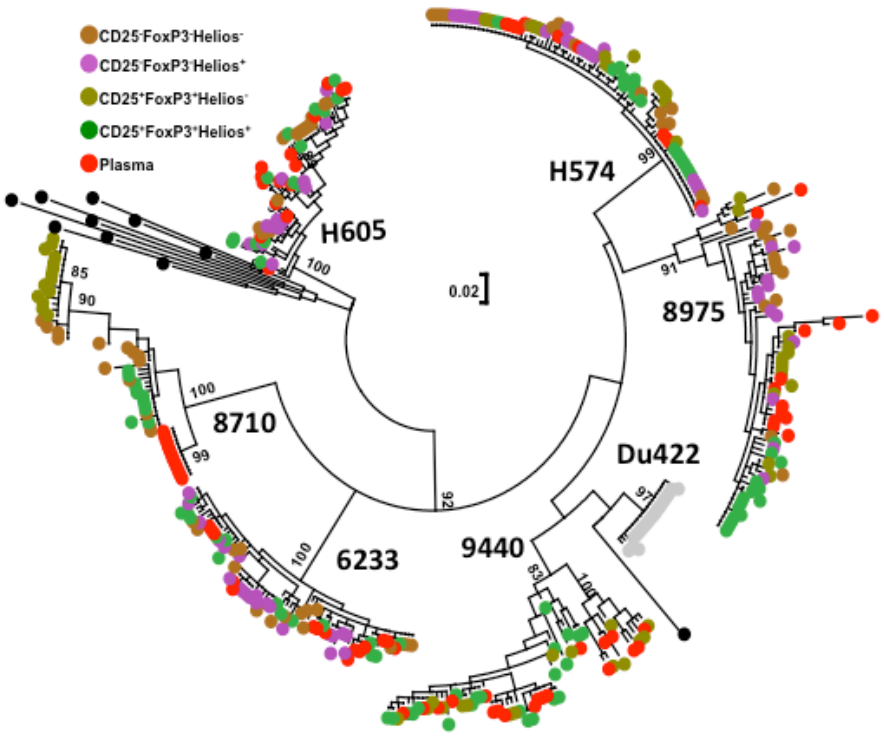
CD25-FoxP3-Helios-
CD25-FoxP3-Helios+
CD25+FoxP3+Helios-
CD25+FoxP3+Helios+
Plasma
H574
H605
8975
8710
Du422
6233
9440
0.02
99
91
85
90
100
100
99
92
97
100
100
83

Figure 5B

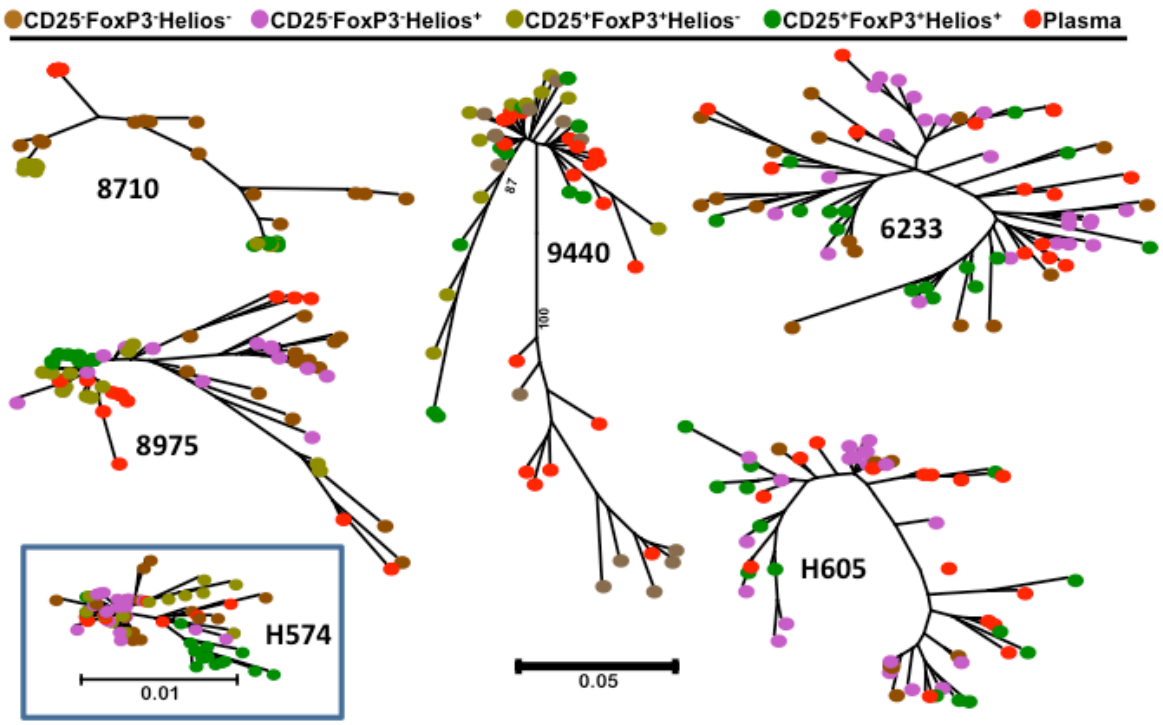
CD25-FoxP3-Helios-
CD25-FoxP3-Helios+
CD25+FoxP3+Helios-
CD25+FoxP3+Helios+
Plasma
8710
9440
6233
8975
H605
H574
87
100
0.01
0.05

Figure 5C

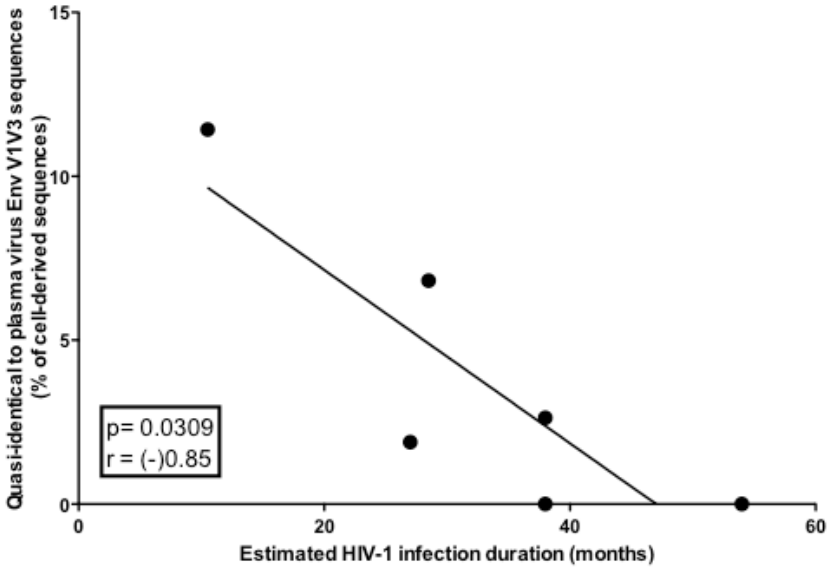

Fig 5. Phylogenetic relationship of HIV Envelope sequences derived from plasma and sorted memory CD4 T cell populations. Plasma- and cell-derived sequences of the highly variable EnvV1V3 region (Hxb 6559–7320) were amplified cloned, sequenced (n=384, Sanger method) and analyzed for 6 viremic subjects with differing HIV infection duration**.** The phylogenetic relationship was inferred by the Maximum Likelihood method based on the General Time Reversible substitution model (GTR+G, **A and B**). Correlation between frequency of cell-derived sequences that were quasi-identical to plasma-derived sequences and the estimated infection duration is shown in (**C**). P and r-values were calculated with the Pearson two-tailed statistical test.